

Experimental fiber optic humidity sensor with applicability to civil structures health monitoring

Sensor experimental de fibra óptica con aplicabilidad al monitoreo de salud de estructuras civiles

Diego H. Alustiza^{1,2,*}, Marcos Mineo¹, Valeria B. Arce^{1,3}, Cristian Villa Pérez^{1,3}, Nélide A. Russo¹

1. Centro de Investigaciones Ópticas (CONICET – CIC – UNLP), Centenario y 506, La Plata, Argentina

2. UTN FRLP, Depto. de Ciencias Básicas, 60 y 124, La Plata, Argentina

3. Departamento de Química, Universidad Nacional de La Plata, Calle 47 y 115, La Plata, Argentina

* E-mail: dalustiza@ciop.unlp.edu.ar

S: miembro de SEDOPTICA / SEDOPTICA member

Received: 29/03/2023

Accepted: 06/06/2023

DOI: 10.7149/OPA.56.2.51138

ABSTRACT:

This paper presents the results obtained in the execution of the first steps of the functional evaluation process of a fiber optic relative humidity sensor. The sensor device was a long period fiber grating (LPG) whose manufacturing process is described. Information is provided on how a humidity sensitivity level was reached that allows relative humidity (RH) measurements to be made. Packaging design implemented is described. Experimental arrangements used for thermal characterization and for humidity response are described. The results are discussed highlighting the details of the experimental setup to be improved in the future. Finally, the conclusions that qualify the feasibility of the implementation of an embedded humidity sensor in concrete structures by using this type of technology are provided.

Key words: structural health monitoring, relative humidity sensor, optical fiber sensor, long period fiber grating

RESUMEN:

En este trabajo se presentan los resultados obtenidos en la ejecución de los primeros pasos del proceso de evaluación funcional de un sensor de humedad relativa implementado en fibra óptica. El dispositivo sensor fue una red de período largo (LPG) cuyo proceso de fabricación es descripto. Se brinda información de cómo se alcanzó un nivel de sensibilidad a la humedad que permita realizar mediciones de humedad relativa (HR). Se describe el diseño del encapsulado implementado. Se finaliza describiendo los arreglos experimentales usados para la caracterización térmica y la determinación del comportamiento del sensor ante un barrido en humedad. Se discuten los resultados resaltando los detalles del arreglo experimental a ser mejorados. Finalmente se brindan las conclusiones que califican la factibilidad de la implementación de un sensor de humedad potencialmente embebible dentro de estructuras de hormigón utilizando este tipo de tecnología.

Palabras clave: monitoreo de salud de estructuras, sensor de humedad relativa, sensor de fibra óptica, red de período largo en fibra óptica

REFERENCES AND LINKS / REFERENCIAS Y ENLACES

- [1] O. E. Gjølrv, «Durability of Concrete Structures,» ARABIAN JOURNAL FOR SCIENCE AND ENGINEERING, vol. 36, p. 151–172, 2011.
- [2] P. Taylor, P. Tennis, K. Obla, P. Ram, T. Van Dam y H. Dylla, «Durability of Concrete, Transportation Research Circular E-C171,» Transportation Research Board, Washington, D.C., 2013



- [3] L. Traversa y Y. A. Villagrán Zaccardi, «INTRODUCCION A LA DURABILIDAD y PATOLOGÍA DE LAS ESTRUCTURAS DE HORMIGON ARMADO,» de IX JORNADA "TECNICAS DE RESTAURACIÓN Y CONSERVACION DEL PATRIMONIO", La Plata, Argentina, 2010.
- [4] A. C. 365, «Service-Life Prediction—State-of-the-Art Report - ACI 365.1R-00,» 2002.
- [5] A. Farhad, Ed., Sensing Issues in Civil Structural Health Monitoring, Springer, 2005.
- [6] X. W. Ye, Y. H. Su y J. P. Han, «Structural Health Monitoring of Civil Infrastructure Using Optical Fiber Sensing Technology: A Comprehensive Review,» The Scientific World Journal, vol. 2014, p. 11, 2014.
- [7] C. I. Merzbacher, A. D. Kersey y E. J. Friebele, «Fiber optic sensors in concrete structures: a review,» Smart Mater. Struct., vol. 5, nº 1996, p. 196-208, 1995.
- [8] B. Glisic y D. Inaudi, FIBRE OPTIC METHODS FOR STRUCTURAL HEALTH MONITORING, John Wiley & Sons Ltd, 2007.
- [9] J. M. López-Higuera, L. Rodriguez Cobo, A. Quintela Incera y , A. Cobo, «Fiber Optic Sensors in Structural Health Monitoring,» JOURNAL OF LIGHTWAVE TECHNOLOGY, vol. 29, nº 4, pp. 587-608, 2011.
- [10] R. Tennyson, T. Coroy, G. Duck, G. Manuelpillai, P. Mulvihill, D. J. Cooper, P. Smith, A. Mufti y S. Jalali, «Fibre optic sensors in civil engineering structures,» Canadian Journal of Civil Engineering, vol. 27, pp. 880-889, 2001.
- [11] M. Sahafnia, «Concrete Structures Durability and Repair,» 2018.
- [12] R. Folić y D. Zenunović, «DURABILITY DESIGN OF CONCRETE STRUCTURES- PART 2: MODELLING AND STRUCTURAL ASSESSMENT,» FACTA UNIVERSITATIS - Series: Architecture and Civil Engineering, vol. 8, nº 1, pp. 45 - 66, 2010.
- [13] A. Méndez, T. F. Morse, F. Méndez, «Applications of embedded optical fiber sensors in reinforced concrete buildings and structures,» Fiber Optic Smart Structures and Skins II, vol. 1170, pp. 60-9.
- [14] D. H. Alustiza, M. Mineo, D. Aredes y N. A. Russo, «Fabricación Local de Sensores de Fibra Óptica Aplicables al Sensado de Magnitudes Relevantes en Ingeniería Civil,» Ingenio Tecnológico, vol. 1, p. 10, 2019.
- [15] D. H. Alustiza, M. Mineo y N. A. Russo, «CHARACTERIZATION OF LONG PERIOD GRATINGS MANUFACTURED WITH FIBER OPTIC FUSION SPLICER FOR SENSOR DEVELOPMENT,» Latin American Applied Research, vol. 51, nº 1, pp. 21-26, 2021.
- [16] D. H. Alustiza, M. Mineo, A. López, Y. A. Villagrán Zaccardi y N. A. Russo, «DESARROLLO DE SENSORES DE FIBRA ÓPTICA PARA LA DETERMINACIÓN DE HUMEDAD EN MEZCLAS CEMENTÍCEAS,» de IX Congreso Internacional y 23ª Reunión Técnica, La Plata, Buenos Aires, Argentina, 2020.
- [17] D. H. Alustiza, M. Mineo, D. Aredes, P. M. D. Gara, V. B. Arce y N. A. Russo, «Sensitivity Improvement of an LPG-based Fiber Optic Humidity Sensor,» IEEE Xplore, p. 5, 2020.
- [18] D. H. Alustiza, M. Mineo, D. Aredes, E. Vaio y N. A. Russo, «Manufacture of Long Period Fiber Gratings for the Development of Optical Sensors,» IEEE Xplore, 2021.
- [19] M. A. Venu Gopal, «Review on Developments in Fiber Optical Sensors and Applications,» International Journal of Materials Engineering, vol. 1, nº 1, pp. 1-16, 2011.
- [20] P. Sharma, S. Pardeshi, R. K. Arora y M. Singh, «A Review of the Development in the Field of Fiber Optic Communication Systems,» International Journal of Emerging Technology and Advanced Engineering, vol. 3, nº 5, pp. 113-119, 2013.
- [21] W. B. Spillman y E. Udd, Field Guide to Fiber Optic Sensors, J. Greivenkamp, Ed., Bellingham, Washington: SPIE, 2014.
- [22] S. Yin, P. B. Ruffin y F. T. S. Yu, Fiber Optic Sensors, B. J. Thompson, Ed., CRC Press, 2008.
- [23] T. L. Yeo, M. A. C. Cox, L. F. Boswell, T. Sun, and K. T. V. Grattan, "Monitoring Ingress of Moisture in Structural Concrete Using a Novel Optical-Based Sensor Approach," Journal of Physics: Conference Series, vol. 45(2006), pp. 186-192, 2006.
- [24] A. J. Swanson, D. Bogunovic, J. Schuyt, Y. Jia, S. Janssens, D. Carder, S. G. Raymond, «Fiber optic relative humidity sensors for use in concrete structures,» The New Zealand Concrete Industry Conference 2017, Te Papa, Wellington, 12 -14 October 2017.

1. Introduction

The temporal evolution of the deterioration produced in reinforced concrete structures due to their interaction with the environment is a topic of great importance and interest for Civil Engineering [1] [2]. The life cycle of any concrete structure is conditioned by the action of agents that cause different processes of gradual degradation in the constituent materials of the structure [3]. The management of the useful life of structures [4] involves preventive maintenance and inspection activities during service phase. In accordance with this, the growing interest in the durable aspects of materials in civil engineering has been accompanied by the development of several structural health monitoring (SHM) techniques during the last decades [5]. In the 1980s and 1990s these techniques, based on the periodic/continuous evaluation of significant indicators of durability, expanded its scope by including optical fiber sensors (OFS) in the measurement system architectures [6] [7] [8] [9].

The benefits obtained by the execution of meticulous monitoring programs of durability indicators based on SHM techniques that imply the use of OFS, show the implementation of a good maintenance management. Engineering actions of this nature are currently considered as crucial activities to prevent the high economic costs normally demanded in rehabilitation campaigns (related to functionality, safety and aesthetics) of reinforced concrete structures, especially large ones. Health monitoring systems installed during the construction phase favor the early detection of some processes related to durability aspects, which implies lower maintenance costs (compared to later detection) [10]. The processed data obtained from the monitoring are used to produce useful information that allows preventing the advance of deleterious processes. For this reason, the early detection of deterioration phenomena not only allows to prolong the useful life of the structure, but also to improve the profitability of the project as a consequence of the reduction of repair costs and the optimization of the structure performance [11] [12].

There are many technical and scientific publications that report different experiences both in the laboratory and in the field, where SHM systems were implemented using OFS. The most registered applications are the monitoring of bridges, buildings, tunnels, gas pipelines, oil pipelines, dams, highways [6]. After the pioneering studies carried out by Méndez et al (1989) [7] suggesting the use of OFS for civil applications, a large number of research groups were formed around the world. The highest degree of development is distributed in the US, some European countries, China, India and Japan. In Argentine there is an evidenced potential for the development and production of these technologies [14] [15] [16] [17] [18], although to date there are no reported cases of application in the field, because the published information is still experimental in nature.

During the last 30 years, an extraordinary evolution of the optoelectronics and the communications industry has been observed. This led to the improvement of the production and quality of the optical components used in communication systems based on the use of optical fiber [19] [20]. The decrease in costs associated with the production of optical components and the appearance of new types of optical fibers caused the growth of the technological fields in which they are applied, resulting in usages outside the field of communications, such as in the field of sensing.

An OFS is essentially a device that allows a physical or chemical agent to interact with the light beam guided within an optical fiber, through a given transduction mechanism. Such interaction manifests itself through the modification of some property of the guided light and it can occur in a spatial region internal or external to the fiber [21]. In the aforementioned context, OFS have become highly competitive options. A certain future projection is observed in which they could displace sensors based on conventional technologies due to their inherent advantages [22]. Recently, they have been favored by the decrease in costs associated with the components used in optical communication systems (optical fiber, light sources, light detectors, beam splitters, connectors, and several other passive components). Actually, this economic issue has been added to the set of benefits of OFS due to both, the communication and sensing systems, share blocks in their respective architectures [21].

The concrete structure interacts with the surrounding environment in different ways during its life cycle. Beyond the interactions for which the structure was designed, there are other interactions that can generate changes in its functional, safety or aesthetic performance. In this context, some environmental agents are considered harmful to concrete because they represent potential causes of damage to the health of the structure (for example, different pathologies can appear due to carbonation processes, chloride and/or sulfate ingress, among others). Also, the presence of water (as liquid or vapor) within the material plays a preponderant role in all transport and degradation phenomena. The knowledge of the

internal humidity level in different strategic places of a concrete structure is a great importance element of judgment for civil engineers when making decisions related to the maintenance of such structures. In this way, monitoring humidity levels provides information that facilitates the implementation of predictive maintenance strategies. This can prevent high levels of economic investment in repairing and retrofitting of structures.

From the physical point of view, water vapor diffuses within the concrete matrix due to a concentration gradient of water molecules content that exists between the environment that surrounds the structure and the core of the material itself. The pores and channels that inherently exist inside of concrete, facilitate the entry of water vapor. Thus, having sensors embedded in the concrete structure to monitor the internal relative humidity (RH) represents a technological resource of great value. In this sense, OFS offer a diverse set of possibilities for the implementation of RH measurements systems.

This paper presents the first steps executed to carry out a functional assessment process for an experimental embeddable humidity OFS potentially applicable to civil structures health monitoring. The sensor is based on the implementation of a specific type of OFS, known as long period fiber grating (LPG).

2. Materials and methods

The detection device consisted of a small optical structure inscribed in an optical fiber. It is a type of diffraction grating, called LPG. It was used as a sensor [23] due to that its optical behavior is sensible to the environment that surrounds it. In this kind of OFS, the operation principle consists in the detection of the wavelength position shift associated to the most prominent attenuation peak (dip) in the light transmission spectrum. This phenomenon occurs due to the fact that its spectral position is sensitive to the fiber surrounding medium refractive index [15]. In this way, variations in amount of water molecules contained in the air that surrounds the fiber produce a small (but detectable) change in the environment refractive index [17]. Due to the fact that the sensor could potentially provide service inside pieces of concrete (that is, the medium that surrounds it will not be air), the design of the encapsulation was carried out in such a way that there is an interface that separates the cementitious material from the space in which LPG is located. Then, the humidification of the air that surrounds the LPG was achieved because the aforementioned interface had channels (conduits) that allowed the exchange of air between the outer space of the encapsulation and the inner space of it.

2.a. Sensor fabrication

In order to construct the sensor as a whole assembly unit, there were executed several fabrication stages. To facilitate the entire performed process description, it will be divided into the following stages: LPG fabrication, humidity functionalizing and packaging assembly. The final physical configuration is shown (in terms of schematically level) in Fig. 1. All the blocks and comments in figure will be explained in following paragraphs according to the stage under description.

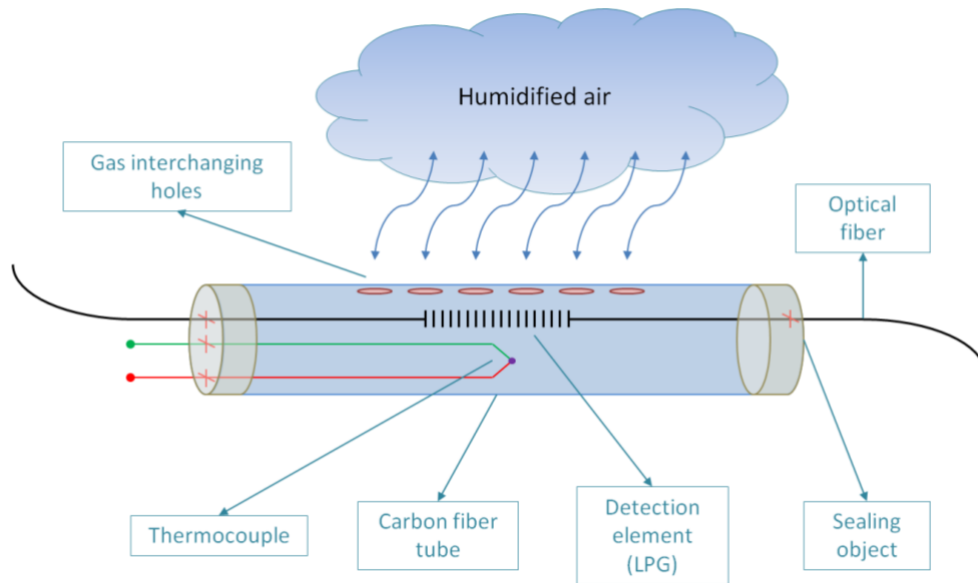


Fig. 1. Final physical configuration scheme for sensor implementation.

2.b. LPG fabrication technique

Like it was mentioned before, the detection effect was based on the employment of an LPG in an optical fiber. In Fig. 1, it is represented with a set of small vertical segments crossing the central zone of the optical fiber (last is represented in black continuous trace).

In order to explain the fabrication technique used, the fundamentals of the LPG structure will be summarized following. In general terms, the formation of an LPG occurs if a succession of changes in the optical fiber effective refractive index is achieved, as it is shown in Fig. 2. It schematizes an optical fiber segment with a series of sections colored in darker gray than the rest of the fiber. That indicates in graphical way the presence of small longitudinal sections where the effective refractive index was intentionally changed. In a LPG like the one used in this work, these small sections are typically distributed forming a uniform pattern along a certain length L . In the context of this manuscript, these small sections will be called “marks”. In the graphical model presented in Fig. 2, all the marks are separated by a fixed distance Λ and the axial extension of each mark is denoted by ℓ .

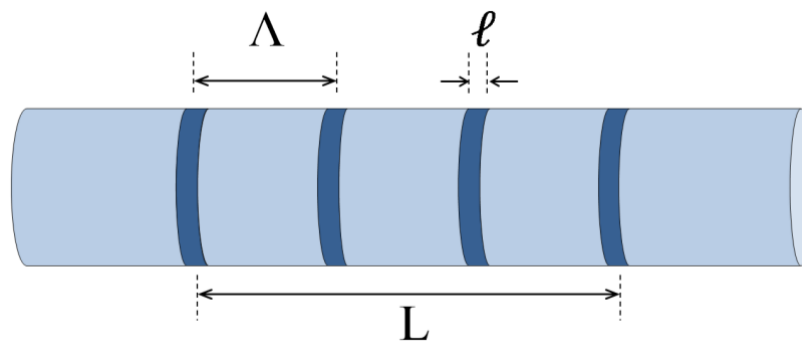


Fig. 2. Longitudinal distribution of a set of marks forming a LPG in an optical fiber.

One way to obtain a mark in some region of the fiber is by generating a controlled deformation known as “microtaper” (from now on, μ -taper). It consists of a decrease in the diameter of the fiber along a given length, usually a few tens of micrometers (for example $100 \mu\text{m}$). In the case of the technique used in this work to generate the μ -tapers, both the diameter of the fiber core and that of the fiber cladding were reduced. Fig. 3 shows schematically a longitudinal view of an optical fiber segment where a μ -taper was generated.

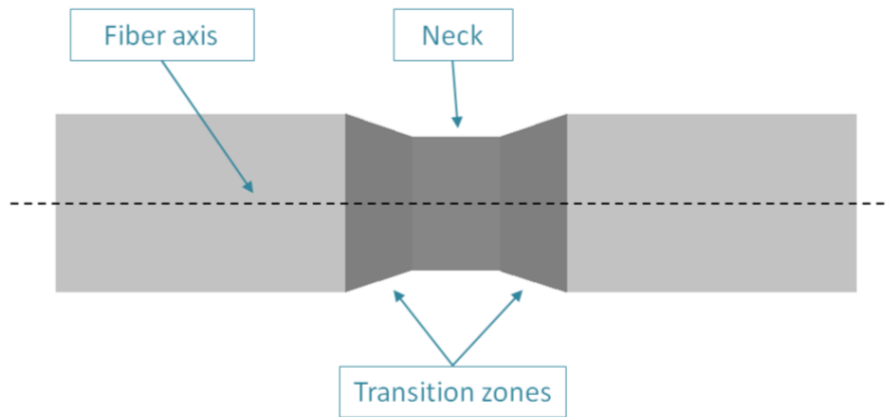


Fig. 3. Graphical model of a μ -taper.

In this work the marks were obtained via implementing two actions: rising up the temperature and stretching the fiber in its axis. This was executed by using a fusion splicer fiber machine (arc induction LPG fabrication technique [14] [15]). A controlled electric arc and a tensile action of specific duration and intensity were used to generate a mark. Then a controlled displacement of the optical fiber was applied. In this way a set of equidistant μ -tapers performed point to point forms the entire LPG. Fig. 4 shows the axial profile of the fiber before (a) and during (b) the application of the electric arc.

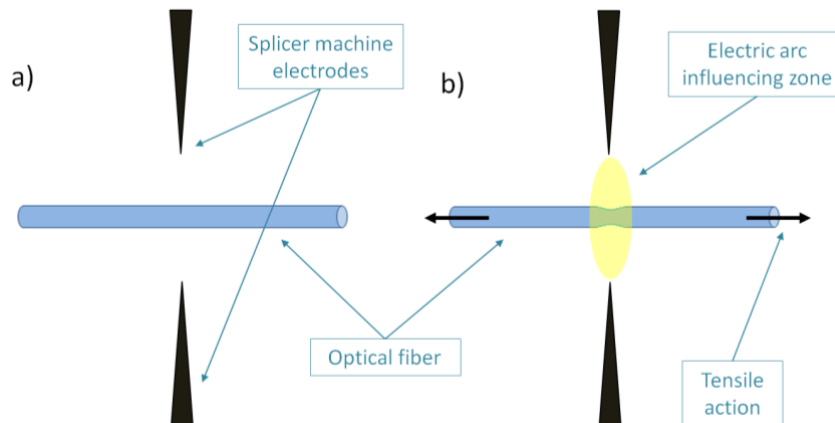


Fig. 4. Optical fiber axial profile before (a) and during (b) electric arc application.

While the electric arc was applied (and in its influence zone), the optical fiber suffered a rise in temperature that exceeded the melting point of the material that constitutes it (silica). As a consequence of the simultaneous application of the axial tension and the electric arc, the fiber suffered a stretching that resulted in the tapering of its longitudinal profile. Once room temperature was reached again, the optical fiber retained the generated deformation showing a reduction in diameter. By applying this technique, reductions between 6% and 9% respect to the original fiber diameter were obtained, which were sufficient to obtain LPG with appropriate optical behavior for its use in sensing applications. Fig. 5 shows the splicer display in which it is observed a μ -taper obtained in laboratory.

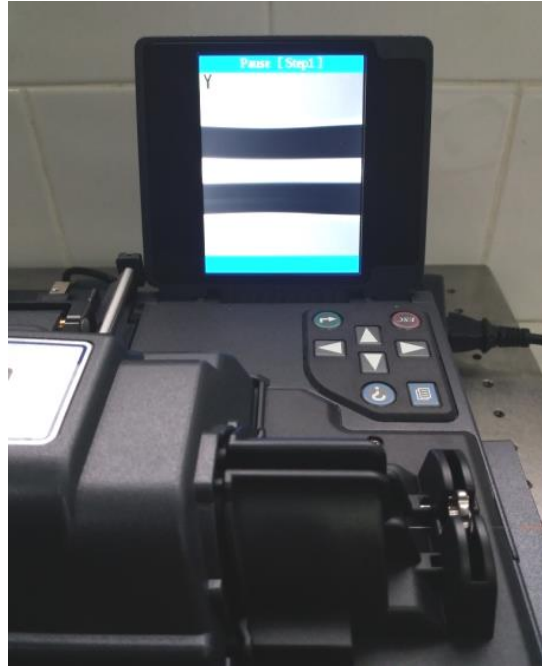


Fig. 5. Splicer display showing a typical μ -taper obtained by applying the described process.

The axial excursion of a typical μ -taper obtained in this way ranged from approximately 100 μm to 120 μm , depending on the environmental conditions present during the forming process (room temperature and room relative humidity).

Fig. 6 shows the experimental setup used for the generation of LPGs. The optical fiber was positioned horizontally in such a way that one end (left) was linked to a mass (M) and the other end (right) was linked to a linear translation stage (T) with a micrometric position control. This allowed the optical fiber to be moved Λ units of length to the right after each electric arc application. The uniformity in the dimensional characteristics of each μ -taper formed was achieved by keeping the parameters related to “arc power”, “attack time” and “traction action” unchanged in each mark of the LPG, as well as an adequate synchronism between them. The mechanical traction intensity equality (from one electric arc attack to the next) was guaranteed by including the mass (M).

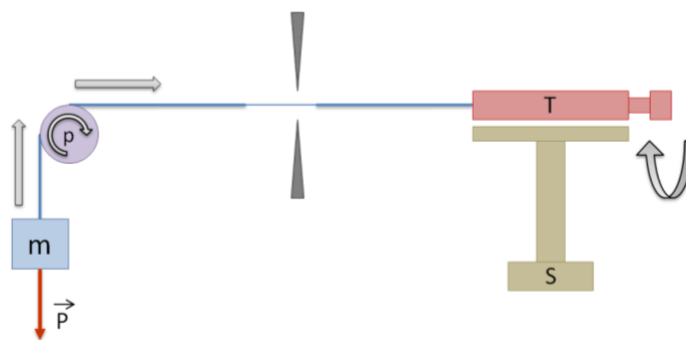


Fig. 6. Experimental setup diagram for LPG fabrication.

The pulley (p) allowed the translation stage to be used in order to reposition the optical fiber after generating each μ -taper. The arrows in Fig. 6 denote the movement direction of the fiber and the position control of T. Finally, the system was aligned through the use of a pedestal of variable height, in such a way that the optical fiber maintains a horizontality that guarantees that its movement does not cause the zone of influence of the electric arc to generate an asymmetric attack on the optical fiber (this could cause micro-bends that distort the geometric uniformity from μ -taper to μ -taper). All these arrangement considerations were reached by means of manual tuning of the experimental setup.

Fig. 7 shows the final physical implementation that is represented by the diagram showed in Fig. 6. The central element is a fiber optic splicer (Fujikura model FSM-100PM) that has two electrodes to generate the electric arc. It also allowed adjustment both the power and the time of electric arc action. The entire experimental set-up was carried out on an optical table from Newport.



Fig. 7. Experimental setup for LPG fabrication. Physical implementation.

It should be noted that such a machine was designed to splice two fiber ends and not to manufacture LPGs. For this reason, each stage of the LPG generation process described in this work was thought to reconcile the original function of the machine with that necessary for the execution of the LPG engraving.

Fig. 8 shows a picture acquired with a Horiba-Jobin Yvon XPlora Plus confocal scanning microscope. For these measurements an optical fiber with a mark was placed on a glass slide, a 10x objective was used. It shows a typical μ -taper obtained by means of the described process execution.

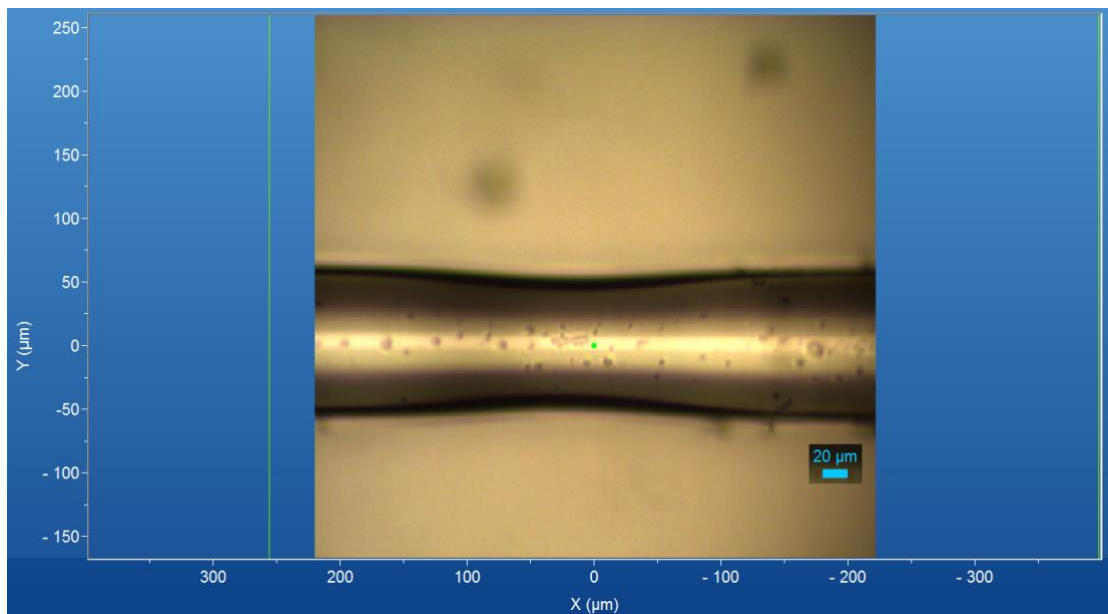


Fig. 8. Segment of an optical fiber where a μ -taper is observed.

The technical characteristics of the optical fiber used in this work are detailed in Table. 1.

TABLE 1. Optical fiber technical characteristics.

| Technical characteristic | Value |
|--------------------------|--------------------------------------|
| Fiber type | SM128 (transmission characteristics) |

| | |
|---------------------------------|---|
| Maximum attenuation (@ 1550 nm) | according to ITU-T G.657.A1, manufactured by Furukawa) |
| Cutoff wavelength | < 0.20 dB/km |
| Mode field diameter (@ 1550 nm) | < 1260 nm |
| Cladding diameter | (10.5 ± 0.8) μm |
| Concentricity core/cladding | (125 ± 1) μm |
| Cladding non-circularity | < 0.5 μm |
| Coating diameter | < 1% |
| Concentricity cladding/coating | (245 ± 5) μm |
| Temperature range | < 12 μm |
| Tensile strength | -60 °C to +85 °C |
| | 100 kpsi |

The LPG optical performance characteristics are listed in Table 2. All measurements were executed in similar environment conditions: room temperature [21.0 ± 0.1] °C; mass acting as tensile action [14.31 ± 0.01] g; RH of the air surrounding the LPG [63% ± 3%]. Dip spectral position, attenuation, bandwidth and insertion loss data are typical values measured over one random specimen from a set of 15 units fabricated using the same technique and under similar laboratory conditions. A typical transmission spectrum of the LPGs generated is shown in Fig. 9.

TABLE 2. Typical LPG optical characteristics.

| Optical characteristic | Value |
|---------------------------------|----------------------------|
| Grating length | (17.050 ± 0.001) mm |
| Grating period | (550 ± 1) μm |
| Prominent dip spectral position | Between 1560 nm to 1570 nm |
| Attenuation @ dip position | > 20 dB |
| Bandwidth | 25 nm approximately |
| Insertion loss | < 3.4 dB @ 1550 nm |

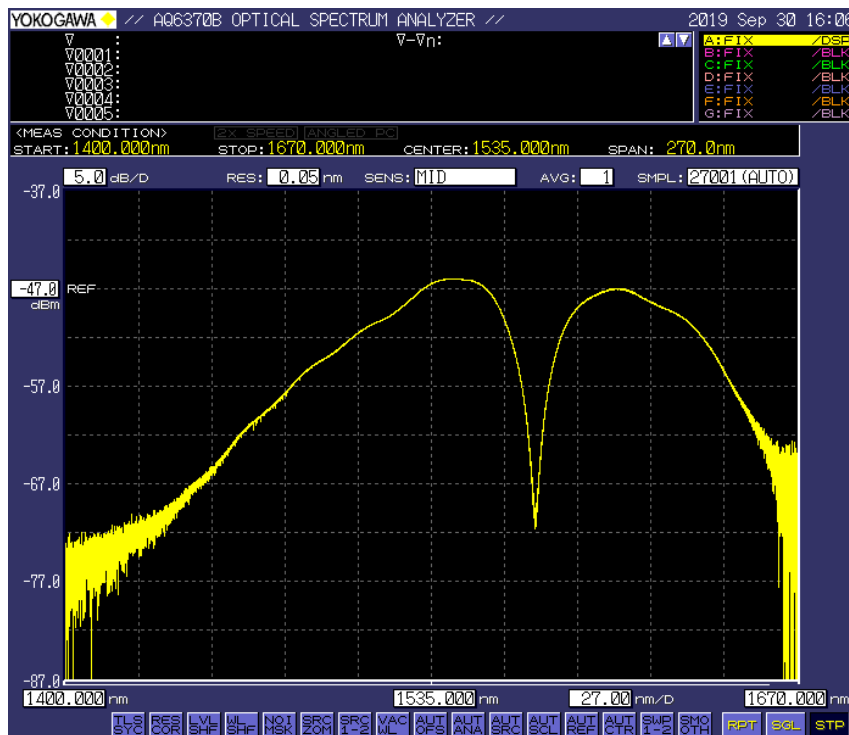


Fig. 9. Typical transmission spectrum of the LPG generated.

2.c. Humidity functionalizing layer

It was observed in laboratory tests that the LPG spectral sensitivity to the change of air humidity level was not high enough to be adequately detected using the available instruments. To strengthen the spectral response to the presence of water in gaseous phase contained in the environmental air surrounding the fiber, a thin functionalizing layer was deposited on the fiber surface (in the zone where the LPG was engraved). The film was constituted by TiO₂ particles due to its strong hydrophilic behavior. To enhance TiO₂ particles adhesion over the LPG (that is, on the optical fiber surface), it was performed a polyurethane (PU) polymeric structure that provided the mechanical support to retain the particles. The deposition process was executed by means of carrying out a set of sequenced stages (immersion in an acetone/PU/TiO₂ mix, drying and curing [7]).

Immersion: the fiber with the engraved LPG was immersed for 30 minutes in a liquid bath of a solution of PU ([2.015 ± 0.001] g) and acetone ([19.087 ± 0.001] g) with dispersed TiO₂ particles ([0.075 ± 0.001] g).

Drying: after removing the fiber from the bath, it was left to rest at room temperature for 60 minutes, thus allowing the evaporation of the liquid phase of the solution.

Curing: the optical fiber was subjected to an oven heating process at 200 °C for approximately 60 minutes. The curing system was implemented using a temperature controller (West2050) and two metal discs with internal grooved surfaces within which the LPG was housed. The two discs that gouged the optical fiber acted as an oven so that their thermal inertia stabilized the temporal behavior of potential sudden variations in temperature.

2.d. Packaging assembly

Concrete is a rustic and potentially aggressive medium (both chemically and mechanically) to embed an optical fiber. This is mainly evidenced during casting the fresh material in moulds and frameworks to produce concrete elements. One way to avoid potential damage to the optical fiber is through the use of a packaging or encapsulation acting as a shield. The main objective is to provide a mechanical protection from the edges and heavy weight of moving aggregates during casting. In addition, the encapsulation ensures that the immediate medium surrounding the fiber was the same (air) as that existing during sensor characterization and calibration.

It can be found a scientific background regarding the implementation of experimental humidity sensors based on the use of fiber optic applicable to concrete [24]. The experiences reached by various research groups around the world were focused on the use of Bragg gratings (FBG) inscribed in optical fiber and protected by metallic encapsulations.

In this work, encapsulation was implemented with a carbon fiber tube. Its dimensional characteristics are summarized in Table 3.

TABLE 3. Carbon fiber tube dimensional characteristics.

| Dimensional characteristic | Value |
|----------------------------|------------------|
| Inner diameter | (4.0 ± 0.2) mm |
| Outer diameter | (6.0 ± 0.2) mm |
| Length | (100.0 ± 0.1) mm |

A linear pattern of 9 circular holes of 1 mm in diameter and approximately 6 mm of spacing from each other was made on the tube. The main function of this orifice arrangement was to provide an exchange path that allows humidified air transport across the interface packaging. The diameter of the holes is such that water in liquid phase does not drain through them due to the developed surface tension. Fig. 10 shows the tube dimensional characteristics and the hole pattern on it.

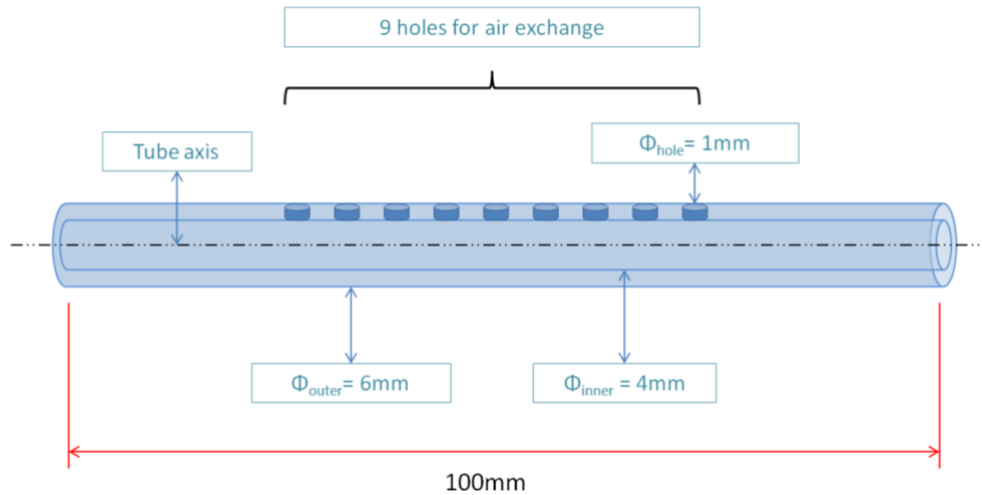


Fig. 10. Carbon fiber tube dimensions and hole pattern location.

As it is shown in Fig. 1, once the optical fiber was threaded into the tube, fastening of the fiber to both extremes of the tube was carried out by applying fast-setting epoxy glue. In addition, the gluing application led to the formation of an enclosure that prevents the entry of water (liquid) through the ends of tube during the embedment in the cementitious matrix (i.e. during fresh state). Fiber fastening was made ensuring that the optical fiber was aligned with the tube axis. Because the spectral response of the LPG is sensitive to the strain suffered by the optical fiber, glue was applied while the fiber was kept under tension using a pulley/mass system to maintain stable axial traction conditions. The used mass was aimed to reproduce the stress situation presented during pre-encapsulation test executed to determine the LPG thermal sensitivity. Fig. 11 shows the physical arrangement used for application of glue to obtain sealed ends.

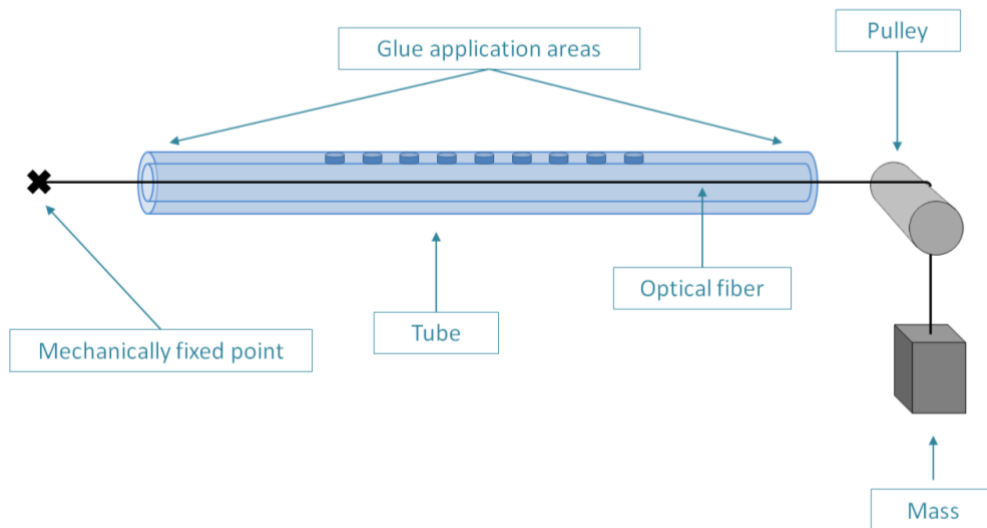


Fig. 11. Packaging ends sealing process setup.

2.e. Mounting frame design

To embed the sensor packaging inside the cement based material specimen tested, it was designed an acrylic structure that is shown in Fig. 12. Its dimensions were compatible with the used mold to guarantee an adequate and proper fit. All the pieces were cut from a 2 mm thick acrylic sheet.

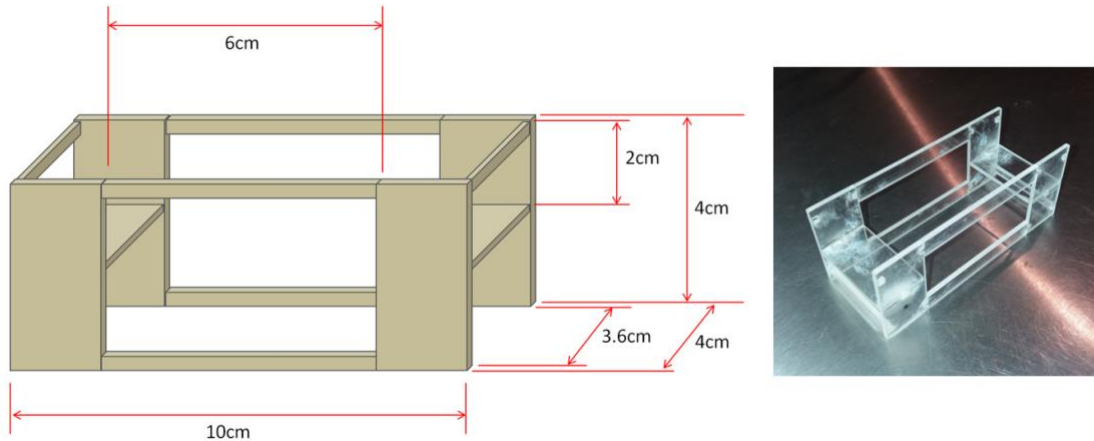


Fig. 12. Mounting frame structure and its dimensions.

To hold and position the sensor packaging on the mounting structure, it was implemented two horizontal planes. These planes provided the supporting surface for the packaging carbon tube. To bond the tube to both planes it was used epoxy glue. Fig. 13 shows a scheme that points how the carbon tube was positioned in the mounting frame structure.

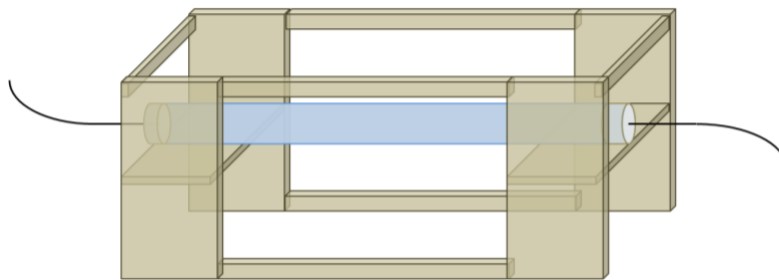


Fig. 13. Packaging carbon tube on the sensor mounting frame structure.

2.f. Thermal shift correction

The spectral position of the attenuation peak in the LPG transmission spectrum is affected by changes in the optical fiber temperature. This behavior tends to mix with the expected one due to the change in humidity of the medium that surrounds the optical fiber. To solve this ambiguous situation a thermocouple (TC) was included inside the packaging. The main purpose of TC inclusion is to determine the air temperature close to the LPG (i.e. inside of the encapsulation and in the nearby region). Knowing the LPG thermal sensitivity, measurements obtained from TC were used to correct for shifts due to thermal changes. The TC was implemented joining two filaments of copper and constantan (T thermocouple type). Joint was carried out via standard tin/copper soldering process. Sensibility obtained over a set of 8 units constructed was (TC thermal sensibility) $(37 \pm 4) \mu\text{V}/^\circ\text{C}$. In the mathematical process applied to the data to execute the thermal correction, $37 \mu\text{V}/^\circ\text{C}$ was used as a typical value.

In its final physical configuration, the TC interrogation port (two wires to be connected to precision voltmeter) was placed in one end of the packaging tube.

2.g. Sensor characterization

Characterization process was performed in two major stages. The first one consisted in the determination of the sensor thermal sensitivity, while the second consisted in a RH environment sweep under controlled laboratory conditions.

As described in a previous section of this manuscript, LPG systems are sensitive to temperature variation. For this reason, to compensate a sensor reading shift due to this sensibility, knowledge about the LPG

thermal behavior was needed. Data obtained in this experimental stage was used to correct dip spectral position due temperature changes occurred during the second stage execution.

Stage 1. Thermal sensitivity determination: to obtain the sensor thermal response, LPG was subjected to a test where a thermal sweep was executed. The optical fiber was confined inside a chamber in which the temperature was controlled by means of a thermal plate system with an accuracy of 0.01°C . Fig. 14 shows experimental setup implemented. This test was performed prior to assemble the packaging. While different stabilized temperature points were achieved, spectral data were saved in a laptop computer linked via Ethernet communication to a spectral optical interrogator (MicronOptics SM125). The last mentioned instrument fed light through the LPG input port, and detected light transmitted through the LPG output port. The experimental arrange is showed in Fig. 15.



Fig. 14. Temperature sweep performed to determine thermal sensitivity.



Fig. 15. Complete experimental setup for thermal sensitivity determination.

Stage 2. RH sensitivity determination: the implementation of the experimental setup took into account the control of several environment influence factors in order to stabilize the measurement conditions. A system specifically designed for the determination of the response of the LPG to changes in the relative humidity of the environment that surrounds it was built. To obtain the response of the LPG to the humidity sweep, the device under test was introduced into a hermetic chamber. Inside it, both the temperature and the humidity of the internal environment were kept under monitoring and control. The chamber was a glass box with an opening on its upper face that has adapted acrylic and wooden covers (removables), fiber optic connectors and the area where the thermal actuator (that was part of the thermal control) was located. Figure 16 shows a diagram of the experimental setup. To keep controlled the temperature, it was used an equipment (TE Technology Inc. CP-200HT model) based on the employment of a thermoelectric cooler. This was linked to an electronic system that, using the measurements performed by interrogating two temperature sensors permanently, commands the thermal

actuator in a PID closed control loop (proportional, integrative, derivative). The thermal actuator (Peltier cell) has the ability to both cool and heat the internal air of the chamber. In addition a cooler (fan) forces the convection of heat, speeding up the thermal energy exchange between the actuator and the internal air of the chamber. The camera takes approximately 30 minutes to stabilize the temperature with a precision that is in the order of 0.01°C . The thermal control guaranteed that the changes observed in the spectral response of the LPGs under test are not strongly due to changes in temperature (magnitude to which all LPG are sensitive). To sense chamber temperature, the thermal control equipment has two NTC type thermistors located in different places inside the chamber. One over the actuator heat exchange plate and the other in a point close to the LPG under test. In addition, an extra temperature monitoring element was added. It was a DHT22 sensor connected to an Arduino Mega 2560 board that allowed recording the internal chamber temperature and humidity on a notebook computer. To keep the tension of the optical fiber constant during each humidity sweep test, a system was implemented by which one end of the fiber was fixed and the other end was subjected to a traction generated by a reference weight (mass/pulley). The internal humidity control was an "open loop" type, which implies the intervention of a human operator. For this, software that runs on Windows was implemented. It allowed operator to view RH and temperature readings measured with the DHT22 sensor located inside the chamber, which gave him information to decide how and when to command the actuators that increase or decrease the internal RH of the chamber. The RH control performance was based on the use of salts saturated solutions that regulate at 11% RH (lithium chloride, LiCl) and 97% (potassium sulfate, K_2SO_4). These regulation values are valid in environments whose temperature is between 5°C and 40°C , a fact that was verified in all the tests carried out. Two plastic trays with the mentioned solutions were housed inside the chamber. The trays had lids whose closing/opening were commanded by an Arduino board through two servomotors/arm mechanisms. The lids of the trays were machined with laser cutting in acrylic plate. A good closure of the covers was ensured through the use of counterweights. The servomotors were driven by firmware downloaded to the Arduino board. It allowed the Arduino to respond to the arrival of serial port commands from the computer in which the user interface software was running. By operating on the lid of the tray that contained the LiCl solution, the internal HR of the chamber was decreased, while operating on its counterpart with K_2SO_4 solution, the HR was increased. The degree of opening of each lid determined the HR value at which the chamber was stabilized. The RH range in which the chamber can potentially stabilize its operating point was approximately 11% to 97%. To improve the dynamic response of the chamber at each HR level in which the system was stabilized, two coolers located near the trays were added. In this way, an internal movement of air was forced to homogenize the humidity of the internal environment of the chamber in approximately 2 minutes for jumps of 1.0% in RH. In order to take each spectral measurement, a lapse of time of 15 minutes was waited after the stability of the chamber was reached at the required operating point (in HR). The test consisted of operating the HR chamber sweeping a given humidity range in steps. Each step represented a stable RH point. Before recording the characteristics of the optical spectrum of the LPG under test, it was verified that the temperature was the same for all measurements carried out (which was established at 22.0°C in the thermal control configuration). Figure 17 shows the laboratory space for the assembly of the experimental arrangement for the execution of the HR sweep tests.

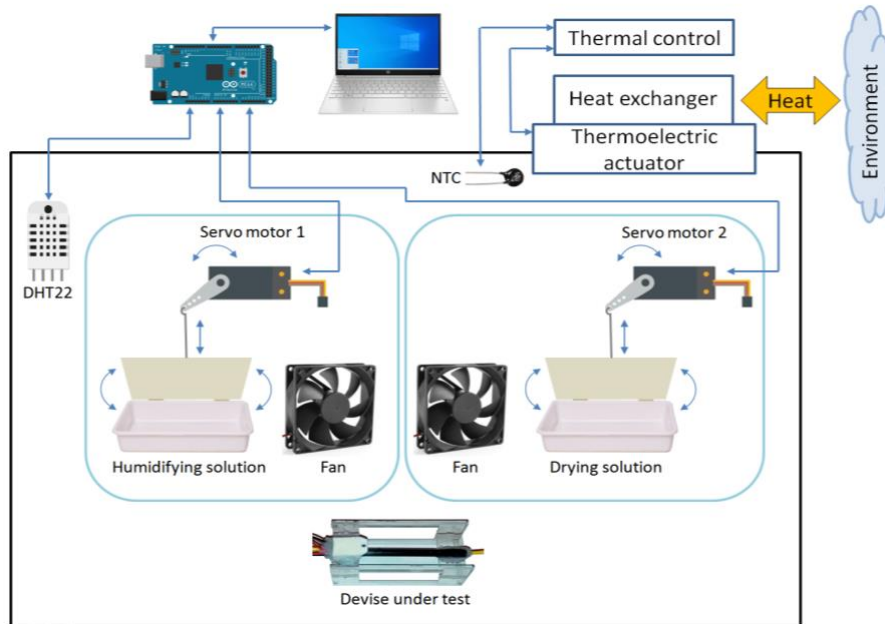


Fig. 16. Experimental set up diagram block for RH sweep test.



Fig. 17. Complete experimental setup for RH sweep and spectral response determination.

3. Data processing

In order to obtain the experimental data that allow establishing the response of the LPG to the humidity of the surrounding medium, the recorded data of the humidity sweep test were processed as follows:

1. To carry out the measurements, an optical spectrum analyzer Yokogawa AQ6370B (OSA) was used (20pm precision).
2. At each humidity stable point reached in the chamber, the spectrum was recorded using a 4.5nm spectral window (wavelength span) and taking 1500 samples.
3. Each sample was averaged 10 times in order to reduce statistical uncertainties.
4. The measured full spectrum was averaged 2 times (roll average).
5. The wavelength of the attenuation peak was determined by searching for the minimum of the function that best visually fit the cloud of experimental points (a polynomial function of degree 5 was chosen, among the options offered by the OSA).
6. The RH measurements uncertainties were $\pm 2\%$ (DHT22).

4. Results

Fig. 18 shows the experimental points obtained during the humidity sweep test for the RH sensitivity determination. The evolution of the spectral position of the LPG attenuation peak is observed, when the HR is varied in the complete test range (33% to 83% approximately). Bars error in red trace and fit function found (and its goodness parameter R) in black trace, are showed.

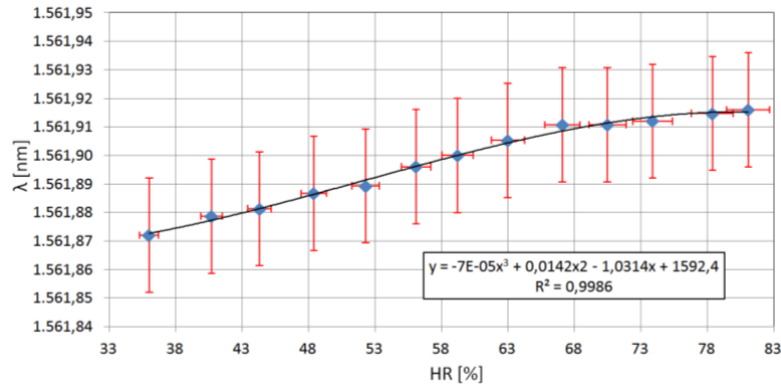


Fig. 18. Attenuation dip spectral [nm] position vs. RH [%].

5. Discussion

This work was oriented to carry out the first steps of an experimental sensor functional assessment process. The complete process should include tests to verify correct sensor operation when it is located inside a cementitious material test specimen (cement paste, mortar, concrete), which will be soon carried out in order to complete the evaluation.

During the thermal characterization test (determination of the LPG sensitivity to temperature) it was assumed that the humidity level remained invariant in the environment close to the fiber. Consequently, the only factor that caused the spectral shift of the dip was the variation in the temperature of the medium.

The implementation of the TC allowed to carrying out the temperature measurement during this evaluation of the sensor. This way of measuring sensor temperature is not appropriate in a concrete embeddable sensor if it is planned to be used in the field. Due to the fact that this way of measuring temperature involves the use electrical principles, remote temperature interrogation requires the use of cables. It enables the system to be sensitive to electromagnetic disturbances and therefore, the measurements are affected by electrical noise. That known effect contradicts the fact of using fiber optics to monitor points of a structure located at great distances from the interrogation system, assuming that the use of light principles is no influenced by electromagnetic interference. To solve this practical issue, it can be implemented a temperature sensor using an LPG inscribed on the same optical fiber that used to implement the humidity sensor. Furthermore, both LPG could share the same package.

It is known that the optical response of the LPG is dependent on changes in the polarization state of the light guided by the fiber. The fiber used in this work was a "single mode" type, so that this sensor is susceptible to being conditioned by changes in both temperature and its mechanical state (both agents that change the birefringence of the fiber, which implies changes in the state of polarization of light in its path). In this work, no studies associated with this topic were carried out, but they will be completed soon in future steps of the evaluation process.

To carry out the humidity sweep test, an OSA (Yokogawa AQ703B) was used. Although the OSA is a low-precision instrument, it is possible to carry out the test with more suitable equipment whose wavelength uncertainties were less than the spectral shifts induced by the changes in RH generated in the chamber.

6. Conclusions

The results of the performance test and the experience acquired in the use of the assembly and calibration guidelines implemented in this work, show that the development of a relative humidity sensor potentially embedded in construction structures is feasible. Although design actions that solve typical practical implementation problems in the field were not carried out yet, the results achieved provide a knowledge base that can be used as the foundations of a technological development project. The technical feasibility analysis of this project, whose objective is the resolution of the practical implementation issues of the experimental fiber optic humidity sensor, can be approached based on the observations made in this work.

Acknowledgements

Authors are grateful to Comisión de Investigaciones Científicas de la Provincia de Buenos Aires (CICPBA) and Agencia Nacional de Promoción de la Investigación, el Desarrollo Tecnológico y la Innovación (Agencia I+D+i) through Fondo para la Investigación Científica y Tecnológica (FONCyT) for the financial support received (CIC Resolutions N° 801/18 and 689/19, N. A. Russo; and PICT 2018-3451, V. B. Arce). The authors thank specially to the CIOp authorities for the support provided.